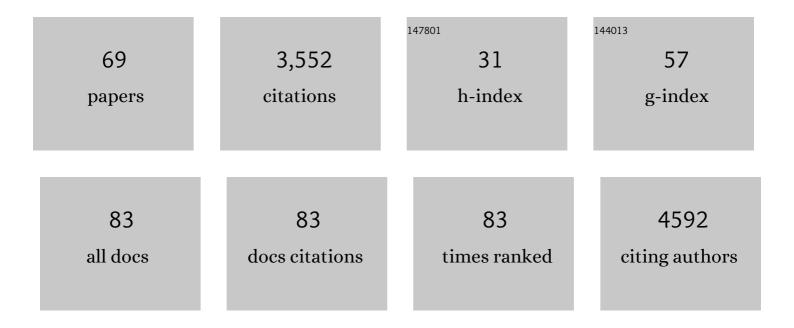
Kaare Teilum

List of Publications by Year in descending order

Source: https://exaly.com/author-pdf/918448/publications.pdf Version: 2024-02-01



KAADE TEILIM

#	Article	IF	CITATIONS
1	Double Mutant of Chymotrypsin Inhibitor 2 Stabilized through Increased Conformational Entropy. Biochemistry, 2022, 61, 160-170.	2.5	6
2	Bidirectional protein–protein interactions control liquid–liquid phase separation of PSD-95 and its interaction partners. IScience, 2022, 25, 103808.	4.1	6
3	Disease-linked mutations cause exposure of a protein quality control degron. Structure, 2022, 30, 1245-1253.e5.	3.3	14
4	Software for reconstruction of nonuniformly sampled NMR data. Magnetic Resonance in Chemistry, 2021, 59, 315-323.	1.9	6
5	Linking thermodynamics and measurements of protein stability. Protein Engineering, Design and Selection, 2021, 34, .	2.1	13
6	Charge Interactions in a Highly Charge-Depleted Protein. Journal of the American Chemical Society, 2021, 143, 2500-2508.	13.7	15
7	Ubiquitin Interacting Motifs: Duality Between Structured and Disordered Motifs. Frontiers in Molecular Biosciences, 2021, 8, 676235.	3.5	6
8	On the specificity of protein–protein interactions in the context of disorder. Biochemical Journal, 2021, 478, 2035-2050.	3.7	41
9	Fitting Side-Chain NMR Relaxation Data Using Molecular Simulations. Journal of Chemical Theory and Computation, 2021, 17, 5262-5275.	5.3	23
10	Synergistic stabilization of a double mutant in chymotrypsin inhibitor 2 from a library screen in E. coli. Communications Biology, 2021, 4, 980.	4.4	13
11	A dual-reporter system for investigating and optimizing protein translation and folding in E. coli. Nature Communications, 2021, 12, 6093.	12.8	12
12	Charge Engineering Reveals the Roles of Ionizable Side Chains in Electrospray Ionization Mass Spectrometry. Jacs Au, 2021, 1, 2385-2393.	7.9	12
13	Global analysis of protein stability by temperature and chemical denaturation. Analytical Biochemistry, 2020, 605, 113863.	2.4	20
14	A highâ€affinity, bivalent <scp>PDZ</scp> domain inhibitor complexes <scp>PICK</scp> 1 to alleviate neuropathic pain. EMBO Molecular Medicine, 2020, 12, e11248.	6.9	20
15	The Determinants for Ligand Binding of the Domesticated Retroviral Protein Arc. Biophysical Journal, 2020, 118, 195a.	0.5	0
16	Binding Revisited—Avidity in Cellular Function and Signaling. Frontiers in Molecular Biosciences, 2020, 7, 615565.	3.5	47
17	Conformational heterogeneity of Savinase from NMR, HDX-MS and X-ray diffraction analysis. PeerJ, 2020, 8, e9408.	2.0	2
18	The Capsid Domain of Arc Changes Its Oligomerization Propensity through Direct Interaction with the NMDA Receptor. Structure, 2019, 27, 1071-1081.e5.	3.3	31

KAARE TEILUM

#	Article	IF	CITATIONS
19	Transient Structural Distortion and Oligomerization of the Capsid Forming Protein Arc is Attenuated by Ligand Binding. Biophysical Journal, 2019, 116, 48a.	0.5	0
20	The three-dimensional structure of an H-superfamily conotoxin reveals a granulin fold arising from a common ICK cysteine framework. Journal of Biological Chemistry, 2019, 294, 8745-8759.	3.4	26
21	Mechanisms of PDZ domain scaffold assembly illuminated by use of supported cell membrane sheets. ELife, 2019, 8, .	6.0	15
22	Towards Improved Biophysical Calculations to Identify Disease-Causing Mutations. Biophysical Journal, 2018, 114, 199a.	0.5	0
23	NCAM2 Fibronectin type-III domains form a rigid structure that binds and activates the Fibroblast Growth Factor Receptor. Scientific Reports, 2018, 8, 8957.	3.3	16
24	Molecular dynamics ensemble refinement of the heterogeneous native state of NCBD using chemical shifts and NOEs. PeerJ, 2018, 6, e5125.	2.0	25
25	(S)Pinning down protein interactions by NMR. Protein Science, 2017, 26, 436-451.	7.6	58
26	The Pathogenic A2V Mutant Exhibits Distinct Aggregation Kinetics, Metal Site Structure, and Metal Exchange of the Cu ²⁺ –Al² Complex. Chemistry - A European Journal, 2017, 23, 13591-13595.	3.3	17
27	Behaviour of intrinsically disordered proteins in protein–protein complexes with an emphasis on fuzziness. Cellular and Molecular Life Sciences, 2017, 74, 3175-3183.	5.4	104
28	Structure of the competence pilus major pilin ComGC in Streptococcus pneumoniae. Journal of Biological Chemistry, 2017, 292, 14134-14146.	3.4	27
29	The extraordinary thermal stability of EstA from <i>S. islandicus</i> is independent of post translational modifications. Protein Science, 2017, 26, 1819-1827.	7.6	8
30	Direct assessment of substrate binding to the Neurotransmitter:Sodium Symporter LeuT by solid state NMR. ELife, 2017, 6, .	6.0	15
31	A Soluble, Folded Protein without Charged Amino Acid Residues. Biochemistry, 2016, 55, 3949-3956.	2.5	34
32	Non-uniform sampling of NMR relaxation data. Journal of Biomolecular NMR, 2016, 64, 165-173.	2.8	33
33	Amyloid-β and α-Synuclein Decrease the Level of Metal-Catalyzed Reactive Oxygen Species by Radical Scavenging and Redox Silencing. Journal of the American Chemical Society, 2016, 138, 3966-3969.	13.7	69
34	Aggregationâ€Prone Amyloidâ€Î²â <cu<sup>II Species Formed on the Millisecond Timescale under Mildly Acidic Conditions. ChemBioChem, 2015, 16, 1293-1297.</cu<sup>	2.6	26
35	Globular and disordered—the non-identical twins in protein-protein interactions. Frontiers in Molecular Biosciences, 2015, 2, 40.	3.5	36
36	Structure of Dimeric and Tetrameric Complexes of the BAR Domain Protein PICK1 Determined by Small-Angle X-Ray Scattering. Structure, 2015, 23, 1258-1270.	3.3	34

KAARE TEILUM

#	Article	IF	CITATIONS
37	relax: the analysis of biomolecular kinetics and thermodynamics using NMR relaxation dispersion data. Bioinformatics, 2014, 30, 2219-2220.	4.1	45
38	Protein Interacting with C-kinase 1 (PICK1) Binding Promiscuity Relies on Unconventional PSD-95/Discs-Large/ZO-1 Homology (PDZ) Binding Modes for Nonclass II PDZ Ligands. Journal of Biological Chemistry, 2014, 289, 25327-25340.	3.4	34
39	Off-resonance rotating-frame relaxation dispersion experiment for 13C in aromatic side chains using L-optimized TROSY-selection. Journal of Biomolecular NMR, 2014, 59, 23-29.	2.8	24
40	The p <i>K</i> _a Value and Accessibility of Cysteine Residues Are Key Determinants for Protein Substrate Discrimination by Glutaredoxin. Biochemistry, 2014, 53, 2533-2540.	2.5	38
41	Helical Propensity in an Intrinsically Disordered Protein Accelerates Ligand Binding. Angewandte Chemie - International Edition, 2014, 53, 1548-1551.	13.8	146
42	Protein Dielectric Constants Determined from NMR Chemical Shift Perturbations. Journal of the American Chemical Society, 2013, 135, 16968-16976.	13.7	82
43	A Folded Excited State of Ligand-Free Nuclear Coactivator Binding Domain (NCBD) Underlies Plasticity in Ligand Recognition. Biochemistry, 2013, 52, 1686-1693.	2.5	39
44	The Human Selenoprotein VCP-interacting Membrane Protein (VIMP) Is Non-globular and Harbors a Reductase Function in an Intrinsically Disordered Region. Journal of Biological Chemistry, 2012, 287, 26388-26399.	3.4	41
45	Is a Malleable Protein Necessarily Highly Dynamic? The Hydrophobic Core of the Nuclear Coactivator Binding Domain Is Well Ordered. Biophysical Journal, 2012, 102, 1627-1635.	0.5	22
46	The WSXWS Motif in Cytokine Receptors IsÂa Molecular Switch Involved in Receptor Activation: Insight from Structures of the Prolactin Receptor. Structure, 2012, 20, 270-282.	3.3	73
47	Millisecond Dynamics in Glutaredoxin during Catalytic Turnover Is Dependent on Substrate Binding and Absent in the Resting States. Journal of the American Chemical Society, 2011, 133, 3034-3042.	13.7	16
48	Remeasuring HEWL pK _a values by NMR spectroscopy: Methods, analysis, accuracy, and implications for theoretical pK _a calculations. Proteins: Structure, Function and Bioinformatics, 2011, 79, 685-702.	2.6	89
49	Rapid Formation of a Preoligomeric Peptide–Metal–Peptide Complex Following Copper(II) Binding to Amyloid βâ€Peptides. Angewandte Chemie - International Edition, 2011, 50, 2532-2535.	13.8	69
50	Protein stability, flexibility and function. Biochimica Et Biophysica Acta - Proteins and Proteomics, 2011, 1814, 969-976.	2.3	178
51	Conformational selection in the molten globule state of the nuclear coactivator binding domain of CBP. Proceedings of the National Academy of Sciences of the United States of America, 2010, 107, 12535-12540.	7.1	152
52	Transient structural distortion of metal-free Cu/Zn superoxide dismutase triggers aberrant oligomerization. Proceedings of the National Academy of Sciences of the United States of America, 2009, 106, 18273-18278.	7.1	74
53	Functional aspects of protein flexibility. Cellular and Molecular Life Sciences, 2009, 66, 2231-2247.	5.4	207
54	Fractional 13C enrichment of isolated carbons using [1-13C]- or [2-13C]-glucose facilitates the accurate measurement of dynamics at backbone Cα and side-chain methyl positions in proteins. Journal of Biomolecular NMR, 2007, 38, 199-212.	2.8	160

KAARE TEILUM

#	Article	IF	CITATIONS
55	Biosynthetic13C Labeling of Aromatic Side Chains in Proteins for NMR Relaxation Measurements. Journal of the American Chemical Society, 2006, 128, 2506-2507.	13.7	76
56	Solution Structures of Human and Porcine β-Microseminoprotein. Journal of Molecular Biology, 2006, 362, 502-515.	4.2	27
57	The inverted chevron plot measured by NMR relaxation reveals a native-like unfolding intermediate in acyl-CoA binding protein. Proceedings of the National Academy of Sciences of the United States of America, 2006, 103, 6877-6882.	7.1	22
58	Different secondary structure elements as scaffolds for protein folding transition states of two homologous four-helix bundles. Proteins: Structure, Function and Bioinformatics, 2005, 59, 80-90.	2.6	51
59	Solution Structure of Human Prolactin. Journal of Molecular Biology, 2005, 351, 810-823.	4.2	105
60	Protein folding: Defining a "standard―set of experimental conditions and a preliminary kinetic data set of two-state proteins. Protein Science, 2005, 14, 602-616.	7.6	207
61	Determination of an Ensemble of Structures Representing the Denatured State of the Bovine Acyl-Coenzyme A Binding Protein. Journal of the American Chemical Society, 2004, 126, 3291-3299.	13.7	155
62	Early kinetic intermediate in the folding of acyl-CoA binding protein detected by fluorescence labeling and ultrarapid mixing. Proceedings of the National Academy of Sciences of the United States of America, 2002, 99, 9807-9812.	7.1	95
63	Transient Intermediary States with High and Low Folding Probabilities in the Apparent Two-state Folding Equilibrium of ACBP at Low pH. Journal of Molecular Biology, 2002, 318, 805-814.	4.2	34
64	Transient Structure Formation in Unfolded Acyl-coenzyme A-binding Protein Observed by Site-directed Spin Labelling. Journal of Molecular Biology, 2002, 324, 349-357.	4.2	85
65	Purification, crystallization and preliminary X-ray diffraction analysis of the carbohydrate-binding domain of flocculin, a cell-adhesion molecule fromSaccharomyces carlsbergensis. Acta Crystallographica Section D: Biological Crystallography, 2002, 58, 2135-2137.	2.5	13
66	Structure of soybean seed coat peroxidase: A plant peroxidase with unusual stability and haem-apoprotein interactions. Protein Science, 2001, 10, 108-115.	7.6	122
67	Arabidopsis ATP A2 peroxidase. Expression and high-resolution structure of a plant peroxidase with implications for lignification. Plant Molecular Biology, 2000, 44, 231-243.	3.9	149
68	Formation of hydrogen bonds precedes the rate-limiting formation of persistent structure in the folding of ACBP. Journal of Molecular Biology, 2000, 301, 1307-1314.	4.2	31
69	Disulfide Bond Formation and Folding of Plant Peroxidases Expressed as Inclusion Body Protein inEscherichia coliThioredoxin Reductase Negative Strains. Protein Expression and Purification, 1999, 15, 77-82.	1.3	17